Inorg. Chem. **2004**, *43*, 1530–1538

Metal vs Ligand Reduction in Complexes of Dipyrido[3,2-*a*:2′,3′-*c*]phenazine and Related Ligands with $[(C_5Me_5)ClM]^+$ (M = Rh or Ir): Evidence for Potential Rather Than Orbital Control in the Reductive Cleavage of the Metal–Chloride Bond

Sascha Berger,[†] Jan Fiedler,[‡] Ralf Reinhardt,[†] and Wolfgang Kaim*,[†]

Institut für Anorganische Chemie, Universität Stuttgart, Pfaffenwaldring 55, D-70550 Stuttgart, Germany, and J. Heyrovský Institute of Physical Chemistry, Academy of Sciences of the Czech Republic, Dolejškova 3, CZ-18223 Prague, Czech Republic

Received October 1, 2003

Complexes between the chlorometal(III) cations $[(C_5Me_5)ClM]^+$, M = Rh or Ir, and the 1,10-phenanthroline-derived α-diimine (N∧N) ligands dipyrido[3,2-*a*:2′,3′-*c*]phenazine (dppz), 1,4,7,10-tetraazaphenanthrene (tap), or 1,10-phenanthroline-5,6-dione (pdo) were investigated by cyclic voltammetry, EPR, and UV–vis–NIR spectroelectrochemistry with respect to either ligand-based or metal-centered (and then chloride-dissociative) reduction. Two low-lying unoccupied molecular orbitals (MOs) are present in each of these three N∧N ligands; however, their different energies and interface properties are responsible for different results. Metal-centered chloride-releasing reduction was observed for complexes of the DNA-intercalation ligands dppz and tap to yield compounds $[(N\wedge N)(C_5Me_5)M]$ in a two-electron step. The separation of α-diimine centered optical orbitals and phenazine-based redox orbitals is apparent from the EPR and UV–vis–NIR spectroelectrochemistry of $[(dppz)(C_5Me_5)M]^{0/\bullet-/2-}$. In contrast, the pdo complexes undergo a reversible one-electron reduction to yield *o*-semiquinone radical complexes $[(pdo)(C_5Me_5)ClM]^\bullet$ before releasing the chloride after the second electron uptake. The fact that the dppz complexes undergo a Cl^--dissociative two-electron reduction despite the presence of a lowest lying π^* MO (b_1(phz)) with very little overlap to the metal suggests that an unoccupied metal/chloride-based orbital is lower in energy. This assertion is confirmed both by the half-wave reduction potentials of the ligands (tap, –1.95 V; dppz, –1.60 V; pdo, –0.85 V) and by the typical reduction peak potentials of the complexes $[(L)(C_5Me_5)ClM](PF_6)$ (tap, –1.1 V; dppz, –1.3 V; pdo, –0.6 V; all values against $Fc^{+/0}$).

Introduction

The reductive heterolysis of a metal−halide bond is a convenient way to generate electronically activated and coordinatively unsaturated species for catalytic purposes. Examples include the α-diimine complexes of $(OC)_3ClRe$ (for CO_2 reduction)[1,2] and of $[(C_5Me_5)ClM]^+$, M = Rh or Ir, which yield intermediate two-electron-reduced complexes with the $[(C_5Me_5)M]$ fragment for the formation and transfer of hydride.[3−6] The use of α-diimine acceptor ligands such as 2,2′-bipyridine raises the question of whether the primary process involves electron uptake by the α-diimine or by the d^6-configurated metal. Whereas the latter, rapidly chloride-releasing two-electron mechanism (1) has been reported for most complex ions $[(N\wedge N)(C_5Me_5)ClM]^+$,[3−6] we have recently shown[7] that the use of the strong π acceptor 2,2′-azobispyridine (abpy) directs the first electron to the acceptor

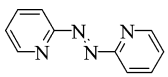

2,2'-azobispyridine
(abpy)

ligand to produce detectable radical complex intermediates

* Author to whom correspondence should be addressed. E-mail: kaim@iac.uni-stuttgart.de.
[†] Universität Stuttgart.
[‡] Academy of Sciences of the Czech Republic.

(1) (a) Hawecker, J.; Lehn, J.-M.; Ziessel, R. *Helv. Chim. Acta* **1986**, *69*, 1900. (b) Sullivan, B. P.; Meyer, T. J. *Organometallics* **1986**, *5*, 1500.
(2) (a) Kaim, W.; Kohlmann, S. *Inorg. Chem.* **1990**, *29*, 2909. (b) Klein, A.; Vogler, C.; Kaim, W. *Organometallics* **1996**, *15*, 236. (c) Scheiring, T.; Klein, A.; Kaim, W. *J. Chem. Soc., Perkin Trans. 2* **1997**, 2569.

10.1021/ic0351388 CCC: $27.50
Published on Web 01/17/2004

(2) before the second electron causes rapid loss of chloride (3).

$$[(N\wedge N)(C_5Me_5)ClM]^+ + 2e^- \xrightarrow{E_{1c}} [(N\wedge N)(C_5Me_5)M] + Cl^- \quad (1)$$

$$[(N\wedge N)(C_5Me_5)M] + Cl^- \xrightarrow{E_{3a}} [(N\wedge N)(C_5Me_5)ClM]^+ + 2e^- \quad (1')$$

$$[(N\wedge N)(C_5Me_5)ClM]^+ + e^- \underset{E_{1a}}{\overset{E_{1c}}{\rightleftharpoons}} [(N\wedge N)(C_5Me_5)ClM]^\bullet \quad (2)$$

$$[(N\wedge N)(C_5Me_5)ClM]^\bullet + e^- \xrightarrow{E_{2c}} [(N\wedge N)(C_5Me_5)M] + Cl^- \quad (3)$$

$$[(N\wedge N)(C_5Me_5)M] + Cl^- \xrightarrow{E_{3a}} [(N\wedge N)(C_5Me_5)ClM]^\bullet + e^- \quad (3')$$

Since abpy is an acceptor ligand[8] with a low reduction potential *and* large LUMO (π^* orbital) coefficients at the metal-coordinating nitrogen atoms (the "metal−ligand interface"[2b]), we became interested in ligand systems which do not exhibit such a parallel combination of orbital energy and composition. Suitable ligands for this purpose are those which form complexes with different "optical" and "redox orbitals".[9,10] Whereas the "redox orbital" is the lowest unoccupied molecular orbital (LUMO) which is populated by the first added electron from a chemical or electrochemical reduction, the "optical orbital" may be higher in energy because it involves the first electronic transition with nonnegligible oscillator strength (band intensity). The lower lying "redox orbital" may just not allow for significant orbital overlap at the metal/ligand interface to effect detectable absorption or emission band intensity.[9,10]

In this report we describe the divergent electron-transfer behavior of complexes between the cations $[(C_5Me_5)ClM]^+$, M = Rh or Ir, and the 1,10-phenanthroline-derived α-diimine ligands dipyrido[3,2-*a*:2′,3′-*c*]phenazine (dppz), 4,7-diaza-1,10-phenanthroline = 1,4,7,10-tetraazaphenanthrene (tap), and 1,10-phenanthroline-5,6-dione (pdo); see Chart 1. dppz is a widely studied ligand,[9−11] often used in complexes aimed at interacting with DNA through intercalation[11a] through which their emission behavior may be significantly altered ("molecular light switch" phenomenon).[9] pdo is the synthetic precursor to dppz;[9−11] it combines a phenanthroline metal chelating site with an *o*-quinone functionality (which can also coordinate to metals, especially in reduced states).[12] Both dppz and dpo are distinguished by having spatially different but energetically close lying π^* orbitals, the lower one being a phenazine (dppz) or *o*-quinone (pdo) centered MO while the higher lying ones are typical α-diimine π^* orbitals of the $b_1(\Psi)$ and $a_2(\chi)$ type[10] (Scheme 1). The latter also pertains to the tap ligand[13] for which detailed studies have established close-lying $b_1(\Psi)$ and $a_2(\chi)$ MOs.[14] The free ligands exhibit quite different half-wave potentials for reversible reduction,

Chart 1

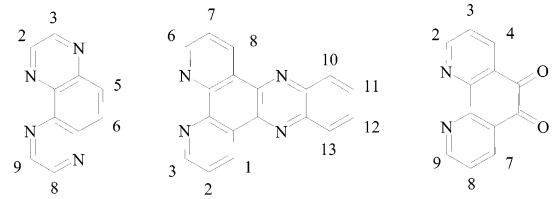

1,4,7,10-tetraaza-phenanthrene (tap) | dipyrido[3,2-*a*:2′,3′-*c*]-phenazine (dppz) | 1,10-phenanthrolin-5,6-dione (pdo)

(3) Kölle, U.; Grätzel, M. *Angew. Chem.* **1987**, *99*, 572; *Angew. Chem., Int. Ed. Engl.* **1987**, *26*, 568.
(4) Chardon-Noblat, S.; Cosnier, S.; Deronzier, A.; Vlachopoulos, N. *J. Electroanal. Chem.* **1993**, *352*, 213.
(5) Caix, C.; Chardon-Noblat, S.; Deronzier, A.; Ziessel, R. *J. Electroanal. Chem.* **1993**, *362*, 301.
(6) (a) Ladwig, M.; Kaim, W. *J. Organomet. Chem.* **1991**, *419*, 233. (b) Ladwig, M.; Kaim, W. *J. Organomet. Chem.* **1992**, *439*, 79. (c) Kaim, W. In *New Trends in Molecular Electrochemistry*; Pombeiro, A. J. L., Ed.; Fontis Media: Lausanne, in press.
(7) Kaim, W.; Reinhardt, R.; Greulich, S.; Fiedler, J. *Organometallics* **2003**, *22*, 2240.
(8) Kaim, W. *Coord. Chem. Rev.* **2001**, *219−221*, 463.
(9) (a) Friedman, A. E.; Chambron, J. C.; Sauvage, J.-P.; Turro, N. J.; Barton, J. K. *J. Am. Chem. Soc.* **1990**, *112*, 4960. (b) Hartshorn, R. M.; Barton, J. K. *J. Am. Chem. Soc.* **1992**, *114*, 5919.
(10) (a) Fees, J.; Kaim, W.; Moscherosch, M.; Matheis, W.; Klima, J.; Krejcik, M.; Zalis, S. *Inorg. Chem.* **1993**, *32*, 166. (b) Fees, J.; Ketterle, M.; Klein, A.; Fiedler, J.; Kaim, W. *J. Chem. Soc., Dalton Trans.* **1999**, 2595. (c) Klein, A.; Scheiring, T.; Kaim, W. *Z. Anorg. Allg. Chem.* **1999**, *625*, 1177. (d) Chambron, J. C.; Sauvage, J.-P.; Amouyal, E.; Koffi, P. *New J. Chem.* **1985**, *9*, 527. (e) Ackermann, M. N.; Interrante, L. V. *Inorg. Chem.* **1984**, *23*, 3904. (f) Arancibia, A.; Concepcion, J.; Daire, N.; Leiva, G.; Loeb, B.; Del Rio, R.; Diaz, R.; Francois, A.; Saldivia, M. *J. Coord. Chem.* **2001**, *54*, 323.
(11) (a) Erkkila, K. E.; Odom, D. T.; Barton, J. K. *Chem. Rev.* **1999**, *99*, 2777. (b) Komatsuzaki, N.; Katoh, R.; Himeda, Y.; Sugihara, H.; Arakawa, H.; Kasuga, K. *J. Chem. Soc., Dalton Trans.* **2000**, 3053. (c) Madureira, J.; Santos, T. M.; Goodfellow, B. J.; Lucena, M.; Pedrosa de Jesus, J.; Santana-Marques, M. G.; Drew, M. G. B.; Félix, V. *J. Chem. Soc., Dalton Trans.* **2000**, 4422. (d) Obare, S. O.; Murphy, C. J. *Inorg. Chem.* **2001**, *40*, 6080. (e) Barker, K. D.; Benoit, B. R.; Bordelon, J. A.; Davis, R. J.; Delmas, A. S.; Mytykh, O. V.; Petty, J. T.; Wheeler, J. F.; Kane-Maguire, N. A. P. *Inorg. Chim. Acta* **2001**, *322*, 74. (f) Liu, J. G.; Zhang, Q.-L.; Shi, X.-F.; Ji, L.-N. *Inorg. Chem.* **2001**, *40*, 5045. (g) Ossipov, D.; Pradeepkumar, P. I.; Holmer, M.; Chattopadhyaya, J. *J. Am. Chem. Soc.* **2001**, *123*, 3551. (h) Önfelt, B.; Lincoln, P.; Nordén, B. *J. Am. Chem. Soc.* **2001**, *123*, 3630. (i) Delaney, S.; Pascaly, M.; Bhattacharya, P. K.; Han, K.; Barton. J. K. *Inorg.. Chem.* **2002**, *41*, 1966. (j) Bilakhiya, A. K.; Tyagi, B.; Paul, P.; Natarajan, P. *Inorg. Chem.* **2002**, *41*, 3830. (k) Metcalfe, C.; Webb, M.; Thomas, J. A. *Chem. Commun.* **2002**, 2026. (l) Rusanova, J.; Decurtins, S.; Rusanov, E.; Stoeckli-Evans, H.; Delahaye, S.; Hauser, A. *J. Chem. Soc., Dalton Trans.* **2002**, 4318. (m) Ossipov, D.; Gohil, S.; Chattopadhyaya, J. *J. Am. Chem. Soc.* **2002**, *124*, 13416. (n) Brennaman, M. K.; Alstrum-Acevedo, J. H.; Fleming, C. N.; Jang, P.; Meyer, T. J.; Papanikolas, J. M. *J. Am. Chem. Soc.* **2002**, *124*, 15094. (n) Yoo, J.; Delaney, S.; Stemp, E..D. A.; Barton, J. K. *J. Am. Chem. Soc.* **2003**, *125*, 6640. (p) Akasaka, T.; Inoue, H.; Kuwabara, M.; Mutai, T.; Otsuki, J.; Araki, K. *Dalton Trans.* **2003**, 815. (q) Metcalfe, C.; Adams, H.; Haq, I.; Thomas, J. A. *Chem. Commun.* **2003**, 1152. (r) Aguirre, P.; Lopez, R.; Villagra, D.; Azocar-Guzman, I.; Pardey, A. J.; Moya, S. A. *Appl. Organomet. Chem.* **2003**, *17*, 36.
(12) (a) Goss, C. A.; Abruña, H. D. *Inorg. Chem.* **1985**, *24*, 4263. (b) Bock, H.; Hänel, P. *Z. Naturforsch., B* **1992**, *47b*, 288. (c) Klein, A.; Kaim, W.; Waldhör, E.; Hausen, H.-D. *J. Chem. Soc., Perkin Trans. 2* **1995**, 2121. (d) Paw, W.; Connick, W. B.; Eisenberg, R. *Inorg. Chem.* **1998**, *37*, 3919. (e) Calderazzo, F.; Pampaloni, G.; Passarelli, V. *Inorg. Chim. Acta* **2002**, *330*, 136. (f) Shavaleev, N. M.; Moorcraft, L. P.; Pope, S. J. A.; Bell, Z. R.; Faulkner, S.; Ward, M. D. *Chem. Commun.* **2003**, 1134. (g) Fujihara, T.; Okamura, R.; Wada, T.; Tanaka, K. *Dalton Trans.* **2003**, 3221.
(13) (a) Ghizdavu, L.; Lentzen; O.; Schumm, S.; Brodkorb, A.; Moucheron, C.; Kirsch-De Mesmaeker, A. *Inorg. Chem.* **2003**, *42*, 1935. (b) Berger, S.; Klein, A.; Kaim, W.; Fiedler, J. *Inorg. Chem.* **1998**, *37*, 5664.
(14) Ernst, S.; Vogler, C.; Klein, A.; Kaim, W.; Zalis, S. *Inorg. Chem.* **1996**, *35*, 1295.

Scheme 1

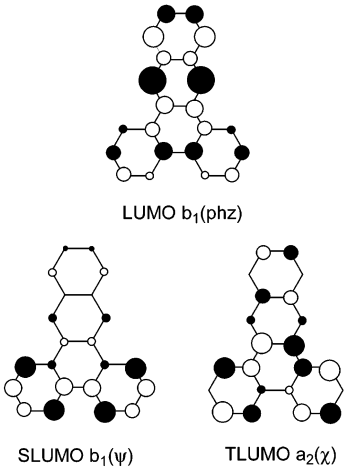

viz., −1.95 V (tap), −1.60 V (dppz), and −0.85 V (pdo), all values vs ferrocene/ferrocenium couple ($Fc^{+/0}$) in *N*,*N*-dimethylformamide/0.1 M Bu_4NPF_6. The electron uptake behavior of the complexes has been investigated using cyclic voltammetry, EPR, and UV/vis spectroelectrochemistry.

Experimental Section

Instrumentation. EPR spectra were recorded in the X band on a Bruker System ESP 300 equipped with a Bruker ER035M gaussmeter and a HP 5350B microwave counter. ^{1}H NMR spectra were taken on a Bruker AC 250 spectrometer. UV−vis−NIR absorption spectra were recorded on Shimadzu UV160 and Bruins Instruments Omega 10 spectrophotometers. Cyclic voltammetry was carried out in *N*,*N*-dimethylformamide (DMF) or in acetonitrile/0.1 M Bu_4NPF_6 using a three-electrode configuration (glassy carbon working electrode, Pt counter electrode, Ag/AgCl reference) and a PAR 273 potentiostat and function generator. The ferrocene/ferrocenium couple ($Fc^{+/0}$) served as internal reference. The setup for rapid-scan cyclovoltammetry was described previously.[7] Simulations of cyclic voltammograms were performed with the program Digisim 2.1 (BAS). Spectroelectrochemical measurements were performed using an optically transparent thin-layer electrolysis (OTTLE) cell[15] for UV/vis spectra and a two-electrode capillary for EPR studies.[16]

[(tap)(C_5Me_5)ClRh](PF_6). A mixture containing 68 mg (0.110 mmol) of $[(C_5Me_5)Cl_2Rh]_2$[17] and 40 mg (0.220 mmol) of tap[13] in 20 mL of acetone was stirred for 15 h. After filtration, addition of 96 mg (0.25 mmol) of Bu_4NPF_6 to the filtrate, and reduction of the volume to about 10 mL, the yellow product precipitated. Washing with diethyl ether and drying under vacuum yielded 105 mg (80%). Anal. Calcd for $C_{20}H_{21}ClF_6N_4PRh$ (600.75): C, 39.99; H, 3.52; N, 9.33. Found: C, 39.73; H, 3.59; N, 9.17%. ^{1}H NMR (CD_3CN): δ = 1.77 (s, 15H, (C_5Me_5)), 8.57 (s, 2H, $H^{5/6}$), 9.30 (dd, 2H, $H^{2/9}$), 9.49 (d, 2H, $H^{3/8}$) ppm; $^3J(H^2H^3/H^8H^9)$ = 2.6 Hz.

[(tap)(C_5Me_5)ClIr](PF_6). The analogous procedure with 65 mg (0.082 mmol) of $[(C_5Me_5)Cl_2Ir]_2$[18] and 30 mg (0.165 mmol) of tap yielded 88 mg (78%) of orange-colored product. Anal. Calcd for $C_{20}H_{21}ClF_6IrN_4P$ (690.06): C, 34.81; H, 3.07; N, 8.12. Found: C, 35.11; H, 3.15; N, 8.18%. ^{1}H NMR (CD_3CN): δ = 1.77 (s, 15H, (C_5Me_5)), 8.60 (s, 2H, $H^{5/6}$), 9.31 (dd, 2H, $H^{2/9}$), 9.46 (d, 2H, $H^{3/8}$) ppm; $^3J(H^2H^3/H^8H^9)$ = 2.7 Hz.

[(pdo)(C_5Me_5)ClRh](PF_6). The analogous procedure with 250 mg (0.40 mmol) of $[(C_5Me_5)Cl_2Rh]_2$ and 255 mg (1.20 mmol) of pdo yielded 350 mg (70%) of yellow product. Anal. Calcd for $C_{22}H_{21}ClF_6N_2O_2PRh$ (628.76): C, 42.03; H, 3.37; N, 4.46. Found: C, 41.94; H, 3.42; N, 4.41%. ^{1}H NMR (CD_3CN)): δ = 1.71 (s, 15H, (C_5Me_5)), 8.04 (dd, 2H, H^5), 8.70 (dd, 2H, H^4), 9.09 (dd, 2H, H^6) ppm; $^3J(H^4,H^5)$ = 8.0, $^3J(H^5,H^6)$ = 5.5, $^4J(H^4,H^6)$ = 1.3 Hz.

[(pdo)(C_5Me_5)ClIr](PF_6). The analogous procedure with 78 mg (0.098 mmol) of $[(C_5Me_5)Cl_2Ir]_2$ and 42 mg (0.200 mmol) of pdo yielded 105 mg (75%) of yellow product. Anal. Calcd for $C_{22}H_{21}ClF_6IrN_2O_2P$ (718.06): C, 36.80; H, 2.95; N, 3.90. Found: C, 36.96; H, 3.17; N, 3.90%. ^{1}H NMR (CD_3CN): δ = 1.70 (s, 15H, (C_5Me_5)), 8.01 (dd, 2H, $H^{3,8}$), 8.69 (dd, 2H, $H^{2,9}$), 9.08 (dd, 2H, $H^{4,7}$) ppm; $^3J(H^2H^3)$ = 8.0, $^3J(H^3H^4)$ = 5.6, $^4J(H^2H^4)$ = 1.4 Hz.

[(dppz)(C_5Me_5)ClRh](PF_6). A suspension of 43 mg (0.068 mmol) of [(pdo)(C_5Me_5)ClRh](PF_6) in 15 mL of ethanol was treated with a ethanolic solution of 9 mg (0.082 mmol) of *o*-phenylenediamine. The color changed from yellow to orange, and after 30 min stirring 5 drops of formic acid were added which results in a slow precipitation. After 15 h the yellow precipitate was collected by filtration and dried under vacuum to yield 80 mg (85%). Anal. Calcd for $C_{28}H_{25}ClF_6N_4PRh$ (700.87): C, 47.98; H, 3.60; N, 7.99. Found: C, 47.66; H, 3.33; N, 7.82%. ^{1}H NMR (CD_3CN): δ = 1.76 (s, 15H, (C_5Me_5)), 8.14 (dd, 2H, $H^{10,13}$), 8.29 (m, 2H, $H^{2,7}$), 8.47 (m, 2H, $H^{11,12}$), 9.32 (dd, 2H, $H^{1,8}$), 9.84 (dd, 2H, $H^{3,6}$) ppm; $^3J(H^7H^8)$ = 8.21, $^3J(H^6H^7)$ = 5.32, $^3J(H^{10}H^{11})$ = 6.52, $^4J(H^{10}H^{12})$ = 3.45, $^4J(H^6H^8)$ = 1.37 Hz.

[(dppz)(C_5Me_5)ClIr](PF_6). The analogous procedure as for [(tap)(C_5Me_5)ClIr](PF_6) with 72 mg (0.092 mmol) of $[(C_5Me_5)Cl_2Ir]_2$ and 52 mg (0.184 mmol) of dppz suspended in 30 mL of acetone yielded 106 mg (73%) of the dark yellow product. Anal. Calcd for $C_{28}H_{25}ClF_6IrN_4P$ (790.18): C, 42.56; H, 3.19; N, 7.09. Found: C, 42.31; H, 3.34; N, 7.11%. ^{1}H NMR (CD_3CN): δ = 1.76 (s, 15H, (C_5Me_5)), 8.15 (dd, 2H, $H^{10.13}$), 8.27 (m, 2H, $H^{2,7}$), 8.48 (m, 2H, $H^{11,12}$), 9.32 (dd, 2H, $H^{1,8}$), 9.80 (dd, 2H, $H^{3,6}$) ppm; $^3J(H^7H^8)$ = 8.23, $^3J(H^6H^7)$ = 5.44, $^3J(H^{10}H^{11})$ = 6.62, $^4J(H^{10}H^{12})$ = 3.44, $^4J(H^6H^8)$ = 1.28 Hz.

Results and Discussion

The complexes [(N∧N)(C_5Me_5)ClM](PF_6) were obtained from the ligands and $[(C_5Me_5)ClM]_2$,[17,18] followed by precipitation with Bu_4NPF_6. Alternatively, the dppz complexes can be obtained from the pdo complexes by condensation with *o*-phenylenediamine. The NMR spectroscopically characterized yellow to orange compounds were subjected to cyclic voltammetry, the results are summarized in Table 1, and representative cyclic voltammograms are shown in Figures 3, 4, and 7.

The tap Complexes. The complexes [(tap)(C_5Me_5)ClM]-(PF_6) show familiar[3−6] behavior according to (1,1′), i.e., a chloride-dissociative two-electron reduction to neutral [(tap)-(C_5Me_5)M] with further quasi-reversible reduction (4) at E_5 to $[(tap)(C_5Me_5)M]^{\bullet-}$ at a much more negative potential ($\Delta E_{1,5} = E_{1c} - E_{5c} \approx 0.85$ V), i.e., at a value similar to that

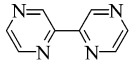
2,2'-bipyrazine
(bpz)

(15) Krejcik, M.; Danek, M.; Hartl, F. *J. Electroanal. Chem.* **1991**, *317*, 179.
(16) Kaim, W.; Ernst, S.; Kasack, V. *J. Am. Chem. Soc.* **1990**, *112*, 173.
(17) Booth, B. L.; Hazeldine, R. N.; Hill, M. *J. Chem. Soc. A* **1969**, 1299.
(18) White, C.; Yates, A.; Maitlis, P. M. *Inorg. Synth.* **1992**, *29*, 228.

Table 1. Peak Potentials of the Complexes [(L)(C_5Me_5)ClM](PF_6)[a]

M/L	E_a(ox)	E_{1c}	E_{1a}	E_{2c}	E_{3a}	E_{5c}	E_{5a}	$\Delta E_{1,5}$[d]	$\Delta E_{1,L}$[e]	$\Delta E_{5,L}$[f]
Rh/tap[b]	+0.57	−1.09			−0.73	−1.96	−1.90	0.87	0.89	0.02
Ir/tap[b]	+0.55	−1.13			−0.69	−1.99	−1.93	0.86	0.85	−0.01
Rh/dppz[b]	n.o.	−1.25			−1.07	−1.70[h]	−1.62	0.45	0.38	−0.07
Ir/dppz[b]	+0.46[g]	−1.31			−1.03	−1.77[i]	−1.69	0.46	0.32	−0.14
Rh/pdo[c]	n.o.	−0.58	−0.50	−1.21	−0.80	−1.50	−1.42	0.92	0.30	−0.62
Ir/pdo[c]	+0.82	−0.62	−0.54	−1.31	−0.90	n.o.	n.o.	n.d.	0.26	n.d.

[a] From cyclic voltammetry at 100 mV/s in 0.1 M Bu_4NPF_6solutions, potentials in V vs $Fc^{+/0}$ (n.o., not observed; n.d., not determined). [b] In DMF. [c] In acetonitrile. [d] $\Delta E_{1,5} = E_{1c} - E_{5c}$. [e] $\Delta E_{1,L} = E_{1c} - E_c$(ligand). [f] $\Delta E_{5,L} = E_{5c} - E_c$(ligand). [g] Reversible process. [h] Further quasi-reversible reduction waves at −2.49, −3.00 V. [i] Further quasi-reversible reduction waves at −2.53, −3.03 V.

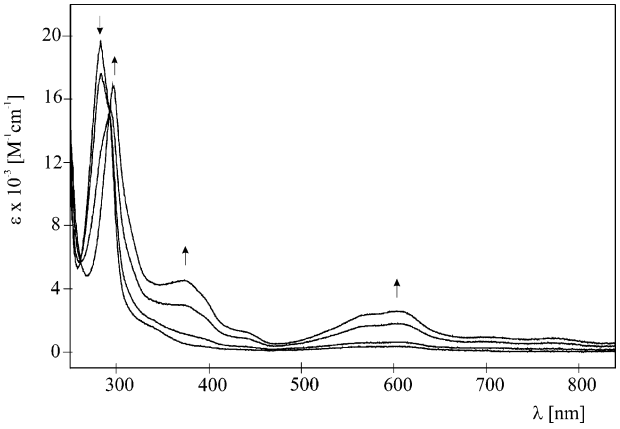

Figure 1. Spectroelectrochemical reduction of tap in DMF/0.1 M Bu_4NPF_6.

of the reduction potential of the free ligand ($\Delta E_{5,L} = E_5 - E_{ligand} \approx 0.0$ V, Table 1). While the first reduction features of the rhodium complex are quite comparable to that of the related [(bpz)(C_5Me_5)ClM](PF_6), bpz = 2,2′-bipyrazine,[6a] the second reduction occurs at a distinctly less negative value, resembing the more facile reduction of the tap ligand (−1.95 vs −2.12 V for bpz). In addition, anodic peak potentials E_a(ox) for irreversible, presumably metal-centered oxidation processes (5) can be determined (Table 1).

$$[(N\wedge N)(C_5Me_5)M] + e^- \underset{E_{5a}}{\overset{E_{5c}}{\rightleftharpoons}} [(N\wedge N)(C_5Me_5)M]^{\bullet -} \quad (4)$$

$$[(N\wedge N)(C_5Me_5)ClM]^+ - e^- \xrightarrow{E_a(ox)} [(N\wedge N)(C_5Me_5)ClM]^{2+} \rightarrow\rightarrow \quad (5)$$

For confirmation of the sequence of (1,1′) we carried out spectroelectrochemical studies of the ligand and of the complex, using an OTTLE cell.[15] Figure 1 shows the effect of the reduction tap → (tap$^{\bullet -}$), and Figure 2 depicts the chloride-releasing two-electron reduction of [(tap)(C_5Me_5)-ClRh](PF_6), yielding [(tap)(C_5Me_5)Rh]. Table 2 summarizes the spectroelectrochemical results.

Reduction to tap$^{\bullet -}$ has been interpreted by EPR spectroscopy to involve the $b_1(\Psi)$ π^* MO with large MO coefficients at the coordinating α-diimine nitrogen centers.[14] The values from Table 2 and Figure 1 confirm this assignment because the main bands in the visible at 604 and 572 nm lie between the values for the related 1,10-phenanthroline radical anion (657 and 604 nm)[19] and 2,2′-bipyrazine radical anion (566 and 531 nm).[20] Weaker bands due to forbidden transitions[20] are found at lower energies.

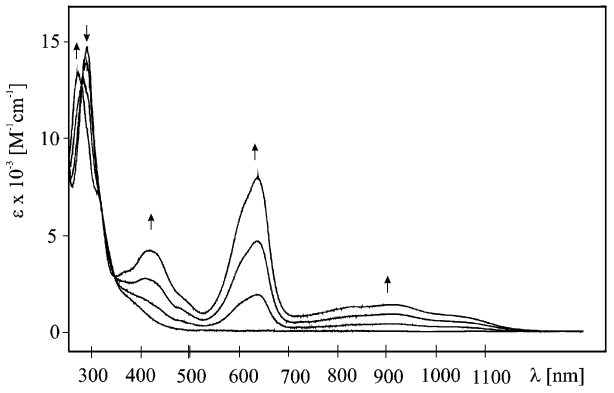

Figure 2. Spectroelectrochemical reduction of [(tap)(C_5Me_5)ClRh](PF_6) in DMF/0.1 M Bu_4NPF_6.

Table 2. UV−vis−NIR Spectroelectrochemical Data of tap and Complexes

	λ_{max} [nm] ($\epsilon \times 10^{-3}$ [M^{-1} cm^{-1}])	
compound	M = Rh	M = Ir
[(tap)(C_5Me_5)ClM]$^+$	290 (14.8) 385sh	288 (18.8) 379 (2.6), 470sh
[tap(C_5Me_5)M]	273 (13.4), 310sh 365sh, 415 (4.3), 490sh 610sh, 635 (7.9) 825sh, 910 (1.5), 1050sh	279 (15.4), 312sh 362 (5.8), 388sh, 448 (5.6) 550sh, 585 (9.8) 725sh, 790 (2.4), 890sh

	λ_{max} [nm] ($\epsilon \times 10^{-3}$ [M^{-1} cm^{-1}])
tap	283 (19), 340sh
tap$^{\bullet -}$	297 (16.8), 370 (5.5), 400sh, 440sh, 572sh, 604 (3.3), 700 (1.6), 780 (1.8)

[a] Measurements from spectroelectrochemistry in 0.1 M Bu_4NPF_6/DMF.

It is clear, however, from Figure 2 and Table 2 that the reduction of the complexes produces the species [(tap)(C_5Me_5)M] which are expected to have intense charge-transfer bands around 600 nm in the visible region arising from transitions between MOs of heavily mixed metal dπ and ligand π^* character.[6,21] The less intense long-wavelength transitions with vibrational fine structuring are due to forbidden transitions involving a partially reduced α-diimine ligand.[6,21]

The dppz Complexes. It could have been anticipated that the particular orbital structure of dppz, involving a lowest lying phenazine-based LUMO b_1(phz), the "redox orbital",

(19) Shida, T. *Electronic absorption spectra of radical ions*; Elsevier: Amsterdam, 1988.
(20) Krejcik, M.; Zalis, S.; Ladwig, M.; Matheis, W.; Kaim, W. *J. Chem. Soc., Perkin Trans. 2* **1992**, 2007.
(21) Zalis, S.; Sieger, M.; Greulich, S.; Stoll, H.; Kaim, W. *Inorg. Chem.* **2003**, *42*, 5185.

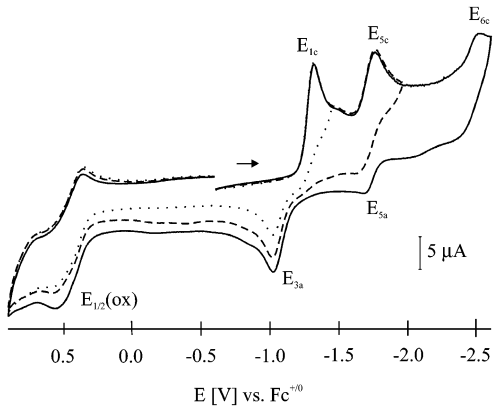

Figure 3. Cyclic voltammograms of 1 mM [(dppz)(C_5Me_5)ClIr](PF_6) in DMF/0.1 M Bu_4NPF_6 at 100 mV/s scan rate.

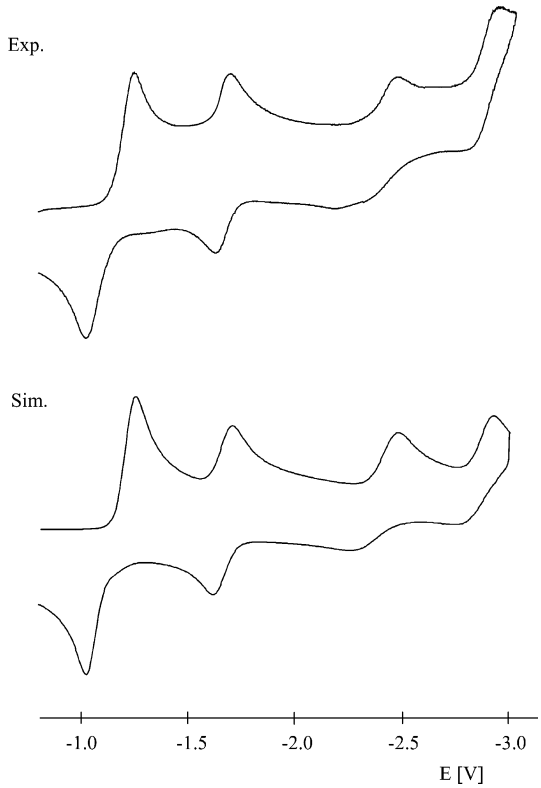

Figure 4. Cyclic voltammogram of 1 mM [(dppz)(C_5Me_5)ClRh](PF_6) in DMF/0.1 M Bu_4NPF_6 at 100 mV/s scan rate with simulation.

and higher lying phenanthroline-type unoccupied MOs[10] of the $b_1(\Psi)$ and $a_2(\chi)$ type,[22] the "optical orbitals", causes a reversible reduction of the corresponding complexes [(dppz)(C_5Me_5)ClM](PF_6). However, as Figures 3 and 4 illustrate, the first reduction is clearly a metal-centered two-electron process with concomitant loss of Cl^-. The main features of the cyclic voltamogram persist also at higher scan rates, up to 10 V/s. For comparison, the complexes [(abpy)(C_5Me_5)ClM](PF_6), abpy = 2,2′-azobispyridine, with a slightly lower ligand reduction potential of −1.37 V, exhibit ligand-based one-electron-reduction intermediates ($E_{red1} \approx -0.5$ V).[7]

The reason for this difference is seen in the still rather negative reduction potential of −1.60 V of free dppz, being shifted to only about −1.30 V in the complexes because of the π^* MO separation between the site of coordination (the α-diimine section) and the potential site of ligand reduction (the phenazine section). Obviously, this insufficient lowering of π^*(dppz) leaves the metal site available for a direct, irreversible (chloride-dissociative) two-electron reduction. The relatively small separation of about 0.25 V between E_{1c} and E_{3a} (1,1′) signifies only a small amount of back-donation in the reduced form.[6]

In agreement with the separated π^* MO situation the second, reversible ligand-centered reduction of the product [(dppz)(C_5Me_5)M] from the chloride-dissociative two-electron reduction occurs at potentials rather close ($\Delta E_{1,5} \approx$ 0.4 V) to those of the first reduction. For the tap complex, this difference ΔE_1 was much larger at about 0.85 V (Table 1), suggesting decoupled MOs in the case of the dppz system. A fourth and fifth electron can be added beyond the state of [(dppz)(C_5Me_5)M]$^{\bullet-}$ to yield highly charged species in irreversible steps; Figure 4 shows a simulation of one corresponding cyclic voltammogram using Scheme 2 and the parameters given in Table 3. Figure 3 shows the quasi-reversible oxidation process of [(dppz)(C_5Me_5)ClIr](PF_6), formally involving an $Ir^{III} \rightarrow Ir^{IV}$ transition.[23]

Scheme 2

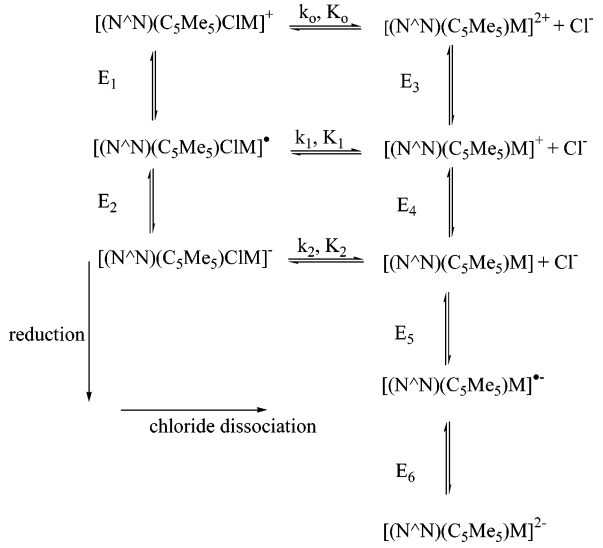

Table 3. Half-Wave Potentials E_i and Constants for Chloride Dissociation of the Complexes [(dppz)(C_5Me_5)ClM](PF_6)[a]

	i						
	1	2	3	4	5	6	7
			M = Rh				
E_i [V] vs $Fc^{+/0}$	−1.23	−1.29	−1.08	−1.10	−1.67	−2.46	−2.97
log k_{i-1} [s^{-1}]	−1.0	1.0	2.0				
log K_{i-1}	−1.8	0.78	4.0				
			M = Ir				
E_i [V] vs $Fc^{+/0}$	−1.29	−1.35	−1.04	−1.07	−1.74	−2.50	−3.00
log k_{i-1} [s^{-1}]	−2.0	1.0	2.0				
log K_{i-1}	−3.0	1.3	6.0				

[a] Pertaining to Scheme 2.Values from computer simulations of cyclic voltammograms at 100 mV/s scan rate, verified to yield good fitting at different scan rates.

(22) Orgel, L. E. *J. Chem. Soc.* **1961**, 3683.

(23) (a) Berger, S.; Baumann, F.; Scheiring, T.; Kaim, W. *Z. Anorg. Allg. Chem.* **2001**, *627*, 620. (b) Greulich, S.; Klein, A.; Knoedler, A.; Kaim, W. *Organometallics* **2002**, *21*, 765.

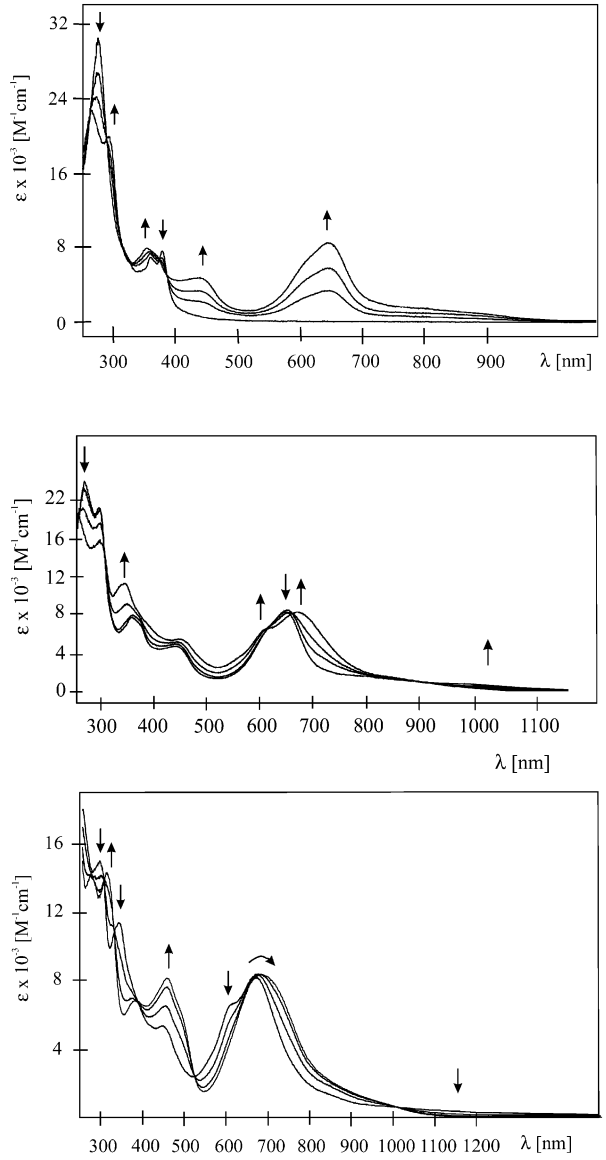

Figure 5. Stepwise (from top to bottom) spectroelectrochemical reduction of [(dppz)(C_5Me_5)ClRh](PF_6) in DMF/0.1 M Bu_4NPF_6.

Remarkably, the (metal-based) first reductions at about −1.30 V lie only slightly less negative than typical potentials of about −1.45 ± 0.1 V for the dppz-centered reduction in complexes (dppz)(ML_n).[10] The (ligand-based) second reductions of [(dppz)(C_5Me_5)ClM](PF_6) at about −1.70 V are only slightly more negative.

The differences $\Delta E_{1,L}$ between the first reduction peak potentials of the complexes and the free ligand are only about 0.3 V, in agreement with the electron addition in an MO (b_1(phz)) having little interaction with the bound metal. The corresponding values were about 0.85 V for the complexes of tap. The differences $\Delta E_{5,L}$ between the reduction potentials of [(dppz)(C_5Me_5)M] and of the free ligand are slightly negative and more so for the iridium analogue, suggesting a small but detectable predominance of metal-to-ligand π back-donation over the coordinative ligand-to-metal σ electron shift.[6,7]

Spectroelectrochemistry (Figure 5, Table 4) confirms the above interpretation (cf. Scheme 2) on the basis of the known

Table 4. Absorption Maxima of dppz and Its Complexes in Different Oxidation States

	λ_{max} [nm] ($\epsilon \times 10^3$ [M^{-1} cm^{-1}])	
compound	M = Rh	M = Ir
[(dppz)(C_5Me_5)ClM]$^+$	280 (31.6)	283 (28.6)
	325sh	325sh
	364 (6.2), 383 (6.8)	365 (6.8), 383sh
[(dppz)(C_5Me_5)M]	268 (23.2), 296 (20.2)	266 (18.0), 288 (17.8)
	358 (7.9)	340sh
	442 (5.2)	400 (6.1)
	610sh, 645 (8.4)	560sh, 594 (11.6), 715 (2.0), 795sh
[(dppz)(C_5Me_5)M]$^{\bullet-}$	298 (15.7)	291 (17.5)
	342 (11.3)	337 (12.0)
	450 (5.6)	397sh, 450sh
	610sh, 672 (8.2), 1000sh	603 (12.2), 625sh, 720 (2.5), 800sh
[(dppz)(C_5Me_5)M]$^{2-}$	314 (14.3), 380 (6.8)	305 (15.0)
	456 (8.2), 495sh	430sh, 450 (8.5)
	605sh, 684 (8.5), 880 (1.9)	603 (10.0), 705 (5.1), 800sh

	λ_{max} [nm] ($\epsilon \times 10^3$ [M^{-1} cm^{-1}])
dppz[b]	290sh, 340 sh, 350sh, 359, 367sh, 379
dppz$^{\bullet-}$ [b]	287, 322, 332sh, 363, 384, 450, 545, 572
dppz^{2-} [b]	287sh, 311sh, 367, 456, 475sh, 719br

[a] From spectroelectrochemistry in 0.1 M Bu_4NPF_6/DMF, [b] From ref 10a.

spectroelectrochemical behavior of dppz.[10] The chloride-dissociative two-electron reduction produces species with intense absorptions around 600−650 nm and also at about 400−450 nm, such as that for [(tap)(C_5Me_5)M]. The structured features at ca. 390 nm associated with largely unperturbed dppz[10a] disappear. Reversible reduction of [(dppz)(C_5Me_5)M] to [(dppz)(C_5Me_5)M]$^{\bullet-}$ produces only slight shifts of the main bands, in agreement with an (EPR-supported) electron uptake by the phenazine-based b_1(phz) "redox" MO which is decoupled from the α-diimine/metal arrangement. Addition of a second electron into b_1(phz) (which is not the "optical orbital") is still not affecting the intense long-wavelength band to a great extent (Figure 5); however, additional features pertaining to the presence of dppz^{2-} appear around 450 nm (Table 4).[10a]

Whereas the one-electron-reduced forms were inaccessible as mentioned above, EPR spectroscopy of the three-electron-reduced forms was possible at room temperature for the rhodium derivative [(dppz)(C_5Me_5)Rh]$^{\bullet-}$. The spectrum in Figure 6 confirms the exclusive localization of the unpaired electron in the b_1(phz) orbital as has been observed similarly for other transition metal complexes (dppz$^{\bullet-}$)(ML_n) (Table 5).[10] The almost invariant g factor and ^{14}N(phenazine) hyperfine splitting illustrate once more the separation of "optical" and "redox" orbitals.

The iridium analogue [(dppz)(C_5Me_5)Ir]$^{\bullet-}$ exhibits an unresolved ESR signal only at 4 K, probably due to rapid relaxation facilitated by the presence of a heavy element and close-lying unoccupied orbitals.[24] EPR silence at ambient temperatures has been observed previously for platinum metal containing radicals.[25]

Again, the marginal deviation of g from the free ligand ion value of 2.0032 confirms the spin location in the b_1-

(24) Kaim, W. *Coord. Chem. Rev.* **1987**, *76*, 187.
(25) Poppe, J.; Moscherosch, M.; Kaim, W. *Inorg. Chem.* **1993**, *32*, 2640.

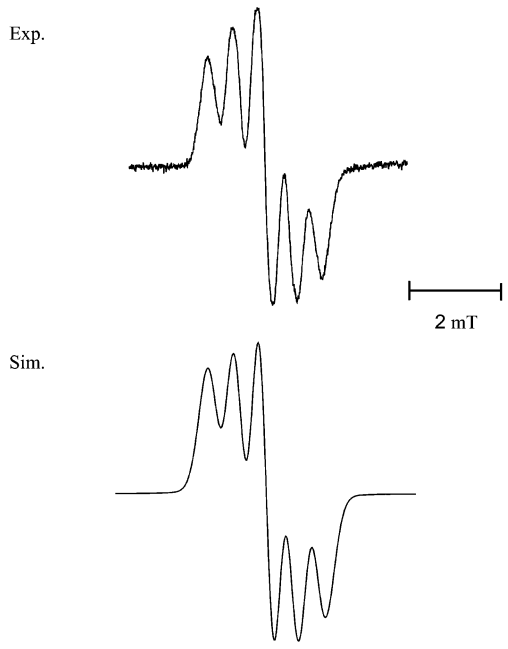

Figure 6. EPR spectrum at 298 K of $[(dppz)(C_5Me_5)Rh]^{\bullet-}$ in DMF/0.1 M Bu_4NPF_6. Computer simulation with the values from Table 5 and 0.44 mT line width (90% Gaussian line shape).

Table 5. EPR Data[a] of $dppz^{\bullet-}$ and Its Complexes

compound	g	$a_N^{(9,14)}$	$a_N^{(4,5)}$	solvent	ref
$dppz^{\bullet-}$	2.0032	0.505	0.021	THF	10a
$[(dppz)(C_5Me_5)Rh]^{\bullet-}$	2.0034	0.53	n.o.	DMF	this work
$[(dppz)(C_5Me_5)Ir]^{\bullet-}$ [b]	2.0030	n.o.	n.o.	DMF	this work
$[(dppz)(bpy)_2Ru]^{\bullet+}$ [46]	2.0034	0.48	0.07	CH_2Cl_2	10a
$[(dppz)(phen)_2Os]^{\bullet+}$ [17,60]	2.0040	0.45	n.o.	CH_3CN	10b
$[(dppz)(CO)_3ClRe]^{\bullet-}$	2.00346	0.497	n.o.	CH_2Cl_2	10b
$[(dppz)(mes)_2Pt]^{\bullet-}$	2.0035	0.52	n.o.	DCE	10b

[a] Coupling constants *a* in mT, electrochemically generated species at 298 K. [b] In glassy frozen solution at 3.7 K.

(phz) orbital. Quite in contrast to these results the EPR spectrum of $[(abpy)(C_5Me_5)Rh]^-$ showed a large *g* anisotropy ($g_1 = 2.161$, $g_2 = 2.002$, $g_3 = 1.945$),[7] suggesting significant metal contribution according to B in eq 6

$$\underset{A}{[(N\wedge N^{\bullet-})(C_5Me_5)Rh^{I}]^-} \leftrightarrow \underset{B}{[(N\wedge N^{2-})(C_5Me_5)Rh^{II}]^-} \qquad (6)$$

However, the decoupling of unoccupied orbitals in dppz clearly favors an alternative A (eq 6) for the complexes of that ligand.

The pdo Complexes. The cyclic voltammograms in Figure 7 illustrate that the complexes $[(pdo)(C_5Me_5)ClM](PF_6)$ exhibit a very different initial reduction behavior from that of the tap and dppz analogues (Table 1).

The first reduction is clearly reversible at potentials of about −0.56 V vs $Fc^{+/0}$, only slightly shifted ($\Delta E_{1,L} \approx 0.3$ V) with respect to the reduction of the free ligand but at much less negative potentials than the chloride-dissociative (metal-centered) reduction of either the tap or the dppz complexes. Here it is the well-separated second reduction step which is irreversible and chloride dissociative (Figure 7). A third electron is taken up by the then formed $[(pdo)(C_5Me_5)M]$ only in a rather irreversible fashion.

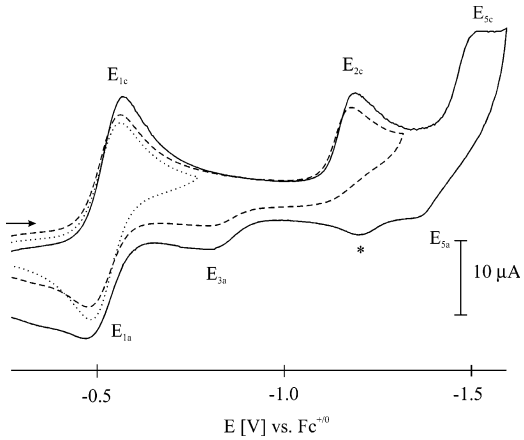

Figure 7. Cyclic voltammograms of 1.7 mM $[(pdo)(C_5Me_5)ClRh](PF_6)$ in CH_3CN/0.1 M Bu_4NPF_6 at 200 mV/s scan rate (*, peak due to unidentified decomposition product).

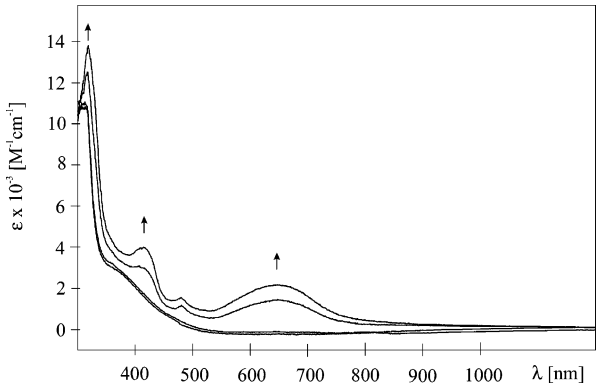

Figure 8. Spectroelectrochemical reduction of $[(pdo)(C_5Me_5)ClRh](PF_6)$ in DMF/0.1 M Bu_4NPF_6.

Spectroelectrochemistry and especially EPR spectroscopy support the interpretation represented by (2), (3), (3′), and (4). The reversible reduction to $[(pdo)(C_5Me_5)ClM]^{\bullet}$ produces new long-wavelength bands at 623 (M = Ir) and 647 nm (M = Rh; Figure 8) which are attributed to intraligand transitions of the coordinated *o*-semiquinone $pdo^{\bullet-}$. Spectroelectrochemically generated free $pdo^{\bullet-}$ has this band at 566 nm, and the related phenanthrene-9,10-semidione has a major absorption maximum at 555 nm.[19] The chloride-free complexes $[(pdo)(C_5Me_5)M]$ (Table 6) exhibit the typical charge-transfer features at 628 nm (M = Ir) or 698 nm (M = Rh).

The *o*-semiquinone character of the one-electron-reduced species is even more clearly evident from the EPR spectra of $[(pdo)(C_5Me_5)ClIr]^{\bullet}$ in fluid and frozen solution (Figures 9 and 10, Table 7).

The hyperfine coupling constants from ^1H and ^{14}N are typically[12b,c] small (<0.15 mT, Table 7) because the spin is concentrated in the semidione moiety of the radical ligand. The ^{14}N splitting of 0.053 mT compares well with 0.06 mT determined for free $pdo^{\bullet-}$ or the 0.0635 mT reported for a diorganoplatinum(II) complex.[12b,c] Similarly, the isotropic *g* value lies in the 2.005 region as expected for semiquinones.[26]

(26) Link, G.; Berthold, T.; Bechtold, M.; Weidner, J. U.; Ohmes, E.; Tang, J.; Poluektov, O.; Utschig, L.; Schlesselman, S. L.; Thurnauer, M. C.; Kothe, G. *J. Am. Chem. Soc.* **2001**, *123*, 4211.

Table 6. UV−vis−NIR Spectroelectrochemical Data of pdo and Its Complexes[a]

compound	λ_{max} [nm] ($\epsilon \times 10^{-3}$ [M^{-1} cm^{-1}]) M = Rh	M = Ir
$[(pdo)(C_5Me_5)ClM]^+$	308 (11)	315 (14.5)
	370 (2.9)	345sh, 415sh
$[(pdo)(C_5Me_5)ClM]^\bullet$	317 (13.9)	310 (17.5)
	404sh, 415 (4.3), 478 (1.7)	418sh, 444 (6.1)
	647 (2.3)	623 (4.6), 695sh
$[(pdo)(C_5Me_5)M]$	320 (13.3)	320sh
	395sh, 415 (4.7)	376 (6.5), 454sh
	698 (4.1)	628 (6.8), 700sh, 775sh

	λ_{max} [nm] ($\epsilon \times 10^{-3}$ [M^{-1} cm^{-1}])
pdo[b]	292, 359
$pdo^{\bullet -}$ [b]	288, 303, 371, 404, 566, 747sh

[a] From measurements in 0.1 M Bu_4NPF_6/DMF. [b] From measurements in 0.1 M Bu_4NPF_6/THF.

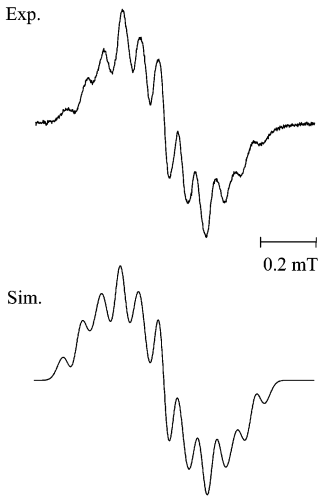

Figure 9. EPR spectrum of $[(pdo)(C_5Me_5)ClIr]^\bullet$ at 298 K in DMF/0.1 M Bu_4NPF_6 with simulation.

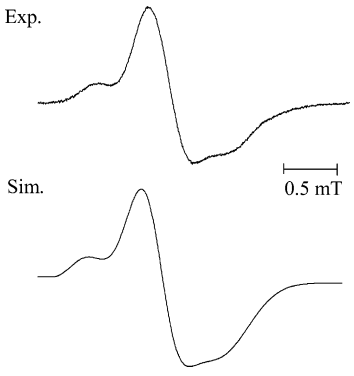

Figure 10. EPR spectrum of $[(pdo)(C_5Me_5)ClIr]^\bullet$ at 110 K in DMF/0.1 M Bu_4NPF_6 with simulation.

However, the determination of the g tensor anisotropy in glassy frozen solution (Figure 10) indicates the effect of the heavy atom coordinating to the spin-bearing semidione site; iridium(III) has a spin−orbit coupling constant of about 4000 cm^{-1}.[27] The g components can be resolved at X-band frequency to yield a total anisotropy $g_1 - g_3 = 0.0099$ which is large in comparison to typical values of about 0.004 for $g_1 - g_3$ in semiquinones.[26]

(27) Weil, J. A.; Bolton, J. R.; Wertz, J. E. *Electron Paramagnetic Resonance*; Wiley: New York, 1994.

Scheme 3

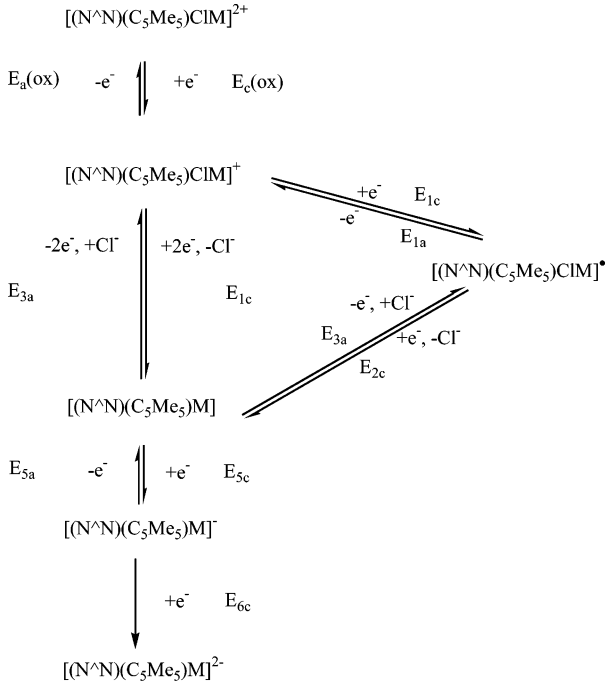

Comparison and Conclusion. With the pdo compounds described here we have found a second example for mononuclear complexes $[(N\wedge N)(C_5Me_5)ClM](PF_6)$ which show reversible one-electron reduction to a radical intermediate before combining with a second electron to effect a metal centered release of chloride. The previous example with N∧N = abpy showed rather high lability of the radical intermediates.[7] In contrast, we have found that the dppz complexes undergo a Cl^--dissociative two-electron reduction just like the tap complexes, despite the presence of a lowest lying π^* MO (b_1(phz)) with very little overlap to the metal. This result suggests that an unoccupied metal/chloride-localized[21] orbital is lower in energy than the ligand π MOs which would be compatible with the electrochemical data obtained. Scheme 3 illustrates the different pathways for the redox reactions of the complexes.

In general, the differences between corresponding rhodium and iridium complexes are rather small, involving the following established[6] trends: Reduction potentials are slightly more negative for the iridium systems which also display larger separations $E_{pa} - E_{pc}$ for the chloride-dissociative process. Oxidation is sometimes found reversible for the $Ir^{III} \rightarrow Ir^{IV}$ transition. Absorption spectroscopy reveals long-wavelength features of the iridium(III) precursor complexes attributed to ^{3}MLCT transitions facilitated through the high spin−orbit coupling constant for the 5d element.[6,21] The intense absorption in the visible attributed to a transition between highly mixed metal and ligand π MOs in $[(N\wedge N)(C_5Me_5)M]$[6,21] is higher in energy for the stronger interacting iridium analogues. The reduced $[(dppz)(C_5Me_5)Ir]^{\bullet -}$ exhibits an ESR spectrum only at very low temperatures due to rapid relaxation.

Table 7. EPR Data of pdo$^{\bullet-}$ and Its Complexes[a]

compound	g_{iso}	g_1[b]	g_2[b]	g_3[b]	Δg[c]	$a(^{14}N)$	$a(H^4)$	$a(H^2)$	solvent	ref
pdo$^{\bullet-}$	2.0050	n.r.	n.r.	n.b.		0.06	0.151	0.110	THF	12b
[(pdo)(C_5Me_5)ClIr]$\bullet$	2.0054	2.0195	2.0094	2.0056	99	0.053	0.149	0.081	DMF	this work
[(pdo) $(mes)_2$Pt]$^{\bullet-}$	2.0045	2.0045	2.0045	2.0045	<20	0.0635	0.120	0.081	THF	12c

[a] Coupling constants a in mT, electrochemically generated at 298 K. [b] At 110 K in glassy frozen solution. [c] $\Delta g = (g_1 - g_3) \times 10^4$.

The potential differences ΔE in Table 1 indicate characteristics for each one of the ligands. The values of $\Delta E_{1,5}$ are smallest for the dppz complexes in agreement with the EPR results that b_1(phz) is still the lowest lying MO in complexes [(dppz)(C_5Me_5)M]. The $\Delta E_{1,L}$ values of the tap systems are large because the $b_1(\Psi)$ π MO with large coefficients at the coordinating α-diimine nitrogen centers is the "redox orbital", strongly affected by metal coordination.[14] The values of $\Delta E_{5,L}$ are most negative for the pdo compounds in agreement[6] with the highest π acceptor capacity.

Acknowledgment. This work was supported by the Deutsche Forschungsgemeinschaft (DFG) and the Fonds der Chemischen Industrie (FCI). We thank Drs. F. Baumann and M. Wanner for measurements of EPR spectra.

IC0351388